Supplymentary Material

Contents

1. Generation of ROS

2. Figure S1. FTIR spectra of EY/UiO-66-NH_2.

3. Figure S2. UV-vis absorption spectra and the corresponding linear fitting of (A) NH_2-H_2BDC molecule absorbance at 366 nm, (B) EY molecule absorbance at 523 nm and (C) UV-vis spectra after digestion procedures for EY/UiO-66-NH_2 (5 mg/mL) with NaOH/DMF(v:v=1:1).

4. Table S1. The feed ratio and actual doping content of EY/UiO-66-NH_2

5. Figure S3. (A) Effect of pH and (B) contact time to the fluorescent intensity ratio I_{533nm}/I_{432nm} of EY/UiO-66-NH_2 suspension.

6. Figure S4. PXRD patterns of EY/UiO-66-NH_2 in PBS (pH=7.4, 10 mM) for different time.

7. Figure S5. Fluorescence intensity ratio I_{533nm}/I_{432nm} of EY/UiO-66-NH_2 after adding different foreign substances in the absence (black) and presence (red) of 10^{-4} mol/L ClO^-.

8. Figure S6. (A) PXRD images and (B) IR spectra and (C) UV/vis spectra and (D) time-resolved fluorescence decays of EY/UiO-66-NH_2 in the presence and absence of 10^{-4} mol/L ClO^-.

9. Figure S7. (A) Fluorescence response of EY (50 μg/mL) toward various ions (10 mM) and (B) toward various ROS species (50 μM (ClO^-, $^1O_2$, $OH\cdot$, $ONOO^-$), 50 mM H_2O_2, 5 mM $O_2^{\cdot-}$). (C) Fluorescence response of EY toward various amount of ClO^-. λ_{ex} = 467 nm, slid width, 1.5 nm/3 nm.

10. Figure S8. Viability of L02, Hela and Raw264.7 cells after incubated with various concentrations of EY/UiO-66-NH_2 after 24 h.

11. Figure S9. Confocal fluorescence imaging of exogenous ClO^- in L02 cells. (A) Bioimaging of

L02 cells without any treatment; (B) Bioimaging of L02 cells incubated with EY/UiO-66-NH_2 (50 μg/mL) for 5 hours at 37°C and (C) further incubated with 100 μM NaClO.

12. Table S2. Comparison of different fluorescence methods for hypochlorite sensing

13. Reference

Generation of ROS

ROS species were obtained according to previous work [1, 2]. ClO^- was diluted from NaClO storage solution. ·OH was prepared by Fenton reaction of Fe^{2+} and H_2O_2 and ·OH has the same concentration as Fe^{2+}. H_2O_2 was acquired from 30% hydrogen peroxide. $O_2^{\cdot -}$ was prepared from pyrogallol autoxidation assay and $^1O_2$ was obtained from the reaction between NaClO and H_2O_2. To prepare ONOO-, sodium sodium nitrite (0.6 M) and hydrogen peroxide (0.7 M) was mixed and the mixture was then acidified with hydrochloric acid solution (0.6 M), following by sodium hydroxide solution (1.5 M) to make the solution alkaline.

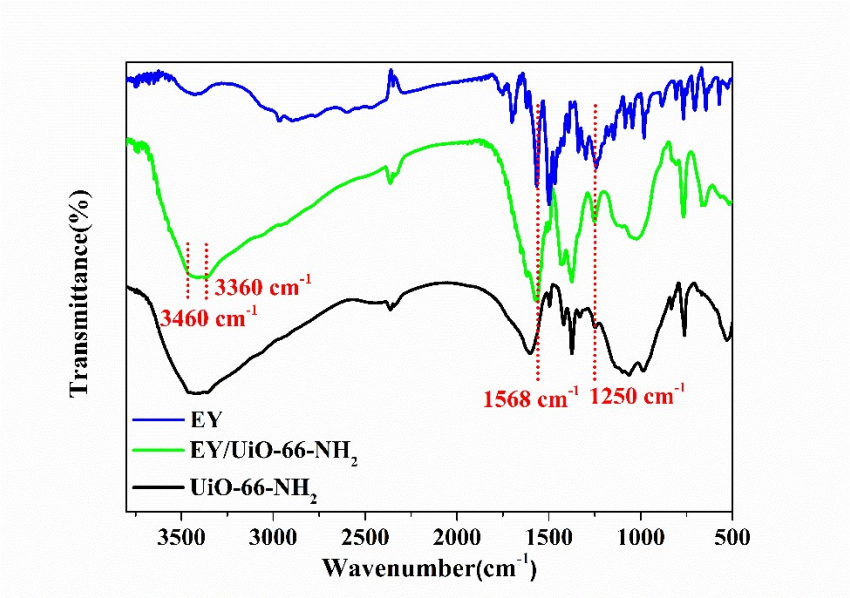

Figure S1. FTIR spectra of EY/UiO-66-NH_2.

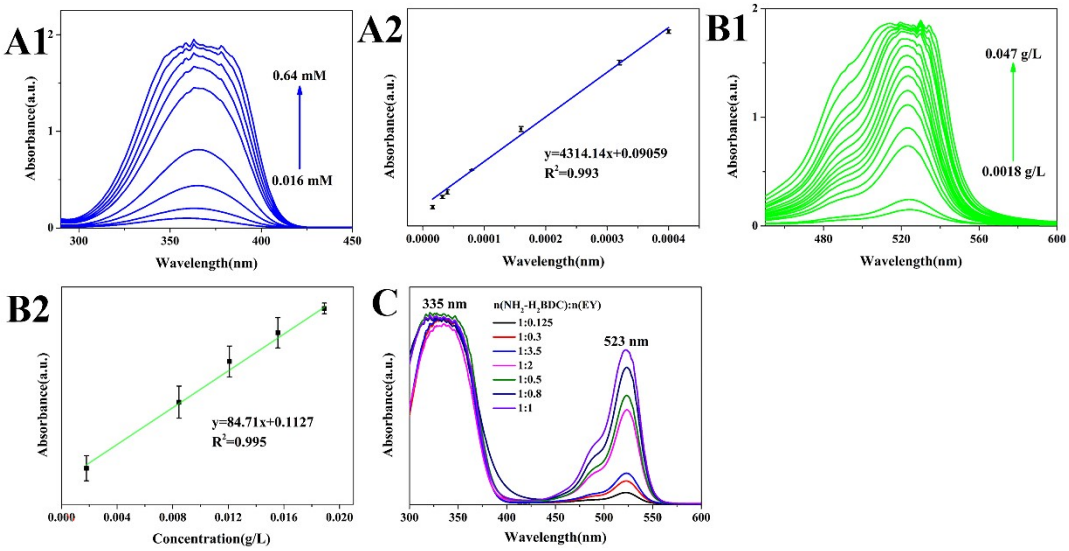

Figure S2. UV-vis absorption spectra and the corresponding linear fitting of (A) NH_2-H_2BDC molecule absorbance at 366 nm, (B) EY molecule absorbance at 523 nm and (C) UV-vis spectra after digestion procedures for EY/UiO-66-NH_2 (5 mg/mL) with NaOH/DMF(v:v=1:1).

Table S1 The feed ratio and actual doping content of EY/UiO-66-NH_2

The feed ratio of EY/UiO-66-NH_2	**Absorbance after digestion and dilution**	**The actual doping content of EY/UiO-66-NH_2**
1:0.125	0.1295	1:0.0013
1:0.3	0.2515	1:0.011
1:0.5	1.1335	1:0.079
1:0.8	1.4429	1:0.068
1:1	1.6061	1:0.12
1:2	0.9857	1:0.1
1:3.5	0.3324	1:0.017

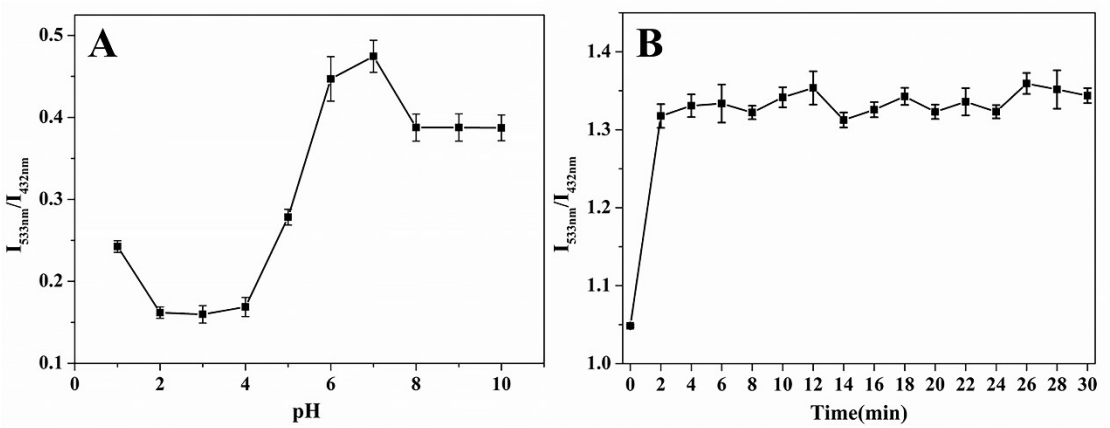

Figure S3. (A) Effect of pH and (B) contact time to the fluorescent intensity ratio I_{533nm}/I_{432nm} of EY/UiO-66-NH_2 suspension.

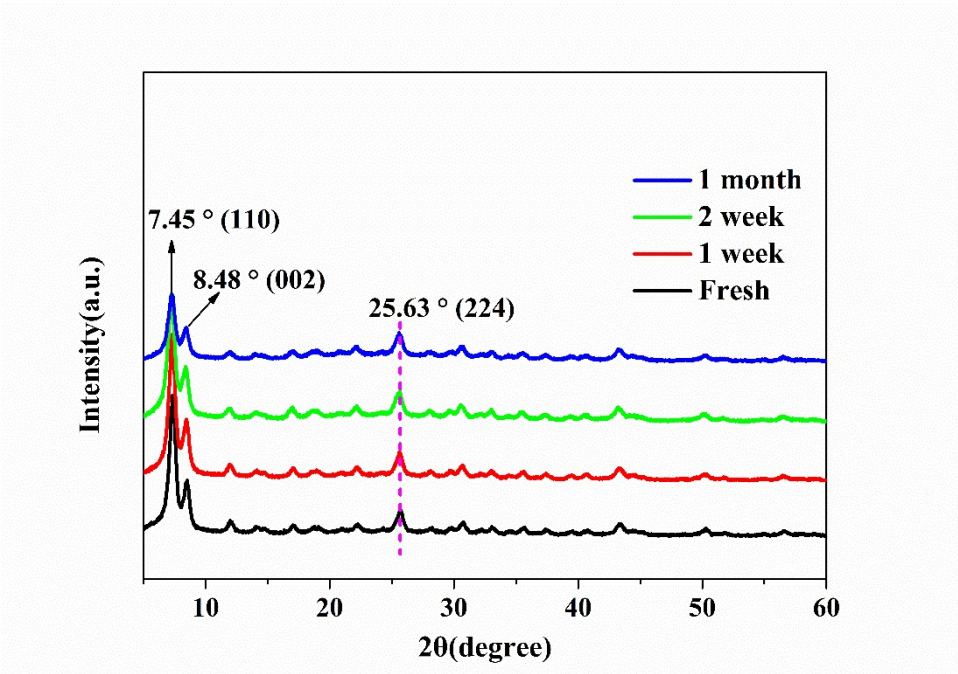

Figure S4. PXRD patterns of EY/UiO-66-NH_2 in PBS (pH=7.4, 10 mM) for different time.

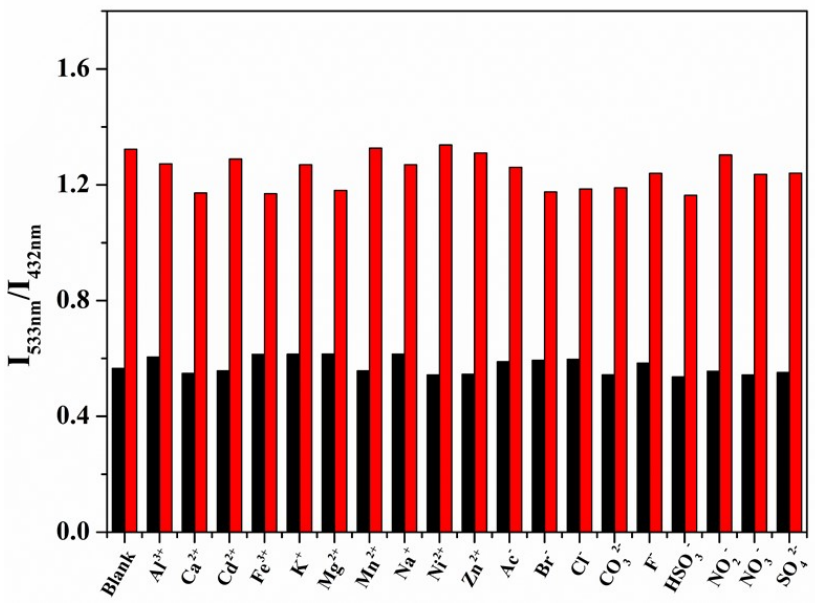

Figure S5. Fluorescence intensity ratio I_{533nm}/I_{432nm} of EY/UiO-66-NH_2 after adding different foreign substances in the absence (black) and presence (red) of 10^{-4} mol/L ClO^-.

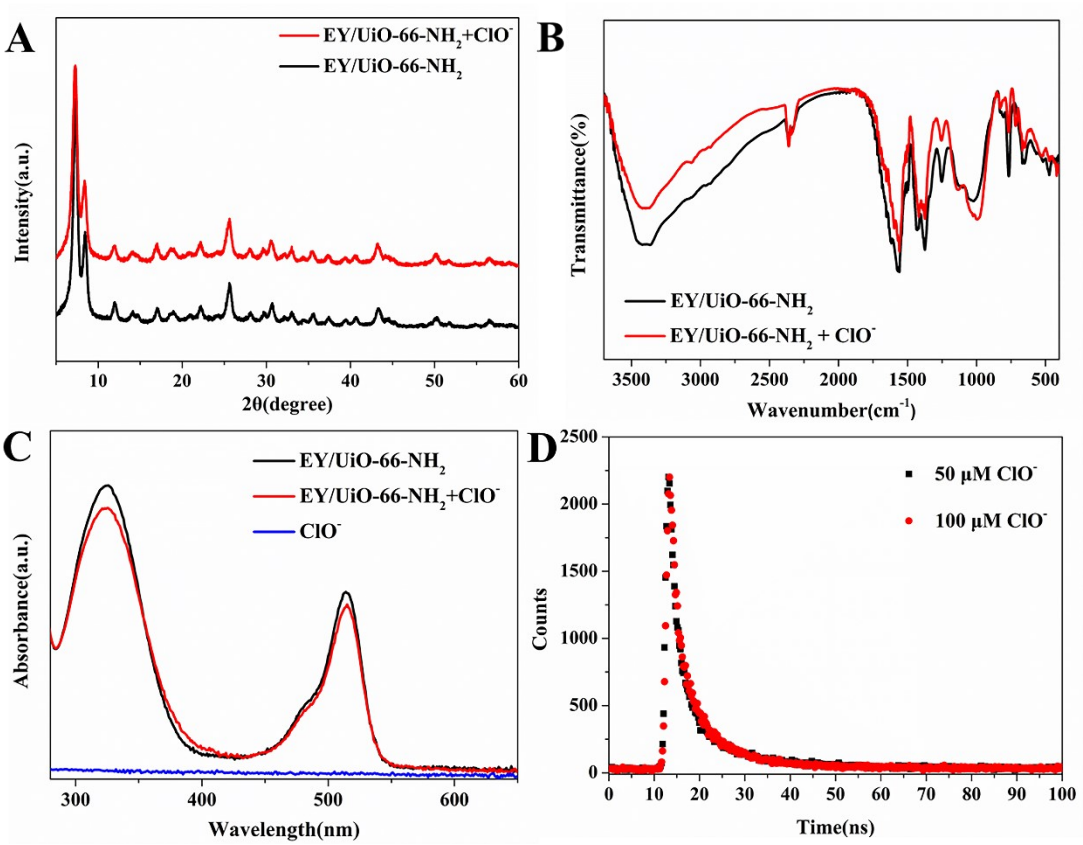

Figure S6. (A) PXRD images and (B) IR spectra and (C) UV/vis spectra and (D) time-resolved

fluorescence decays of EY/UiO-66-NH_2 in the presence and absence of 10^{-4} mol/L ClO^-.

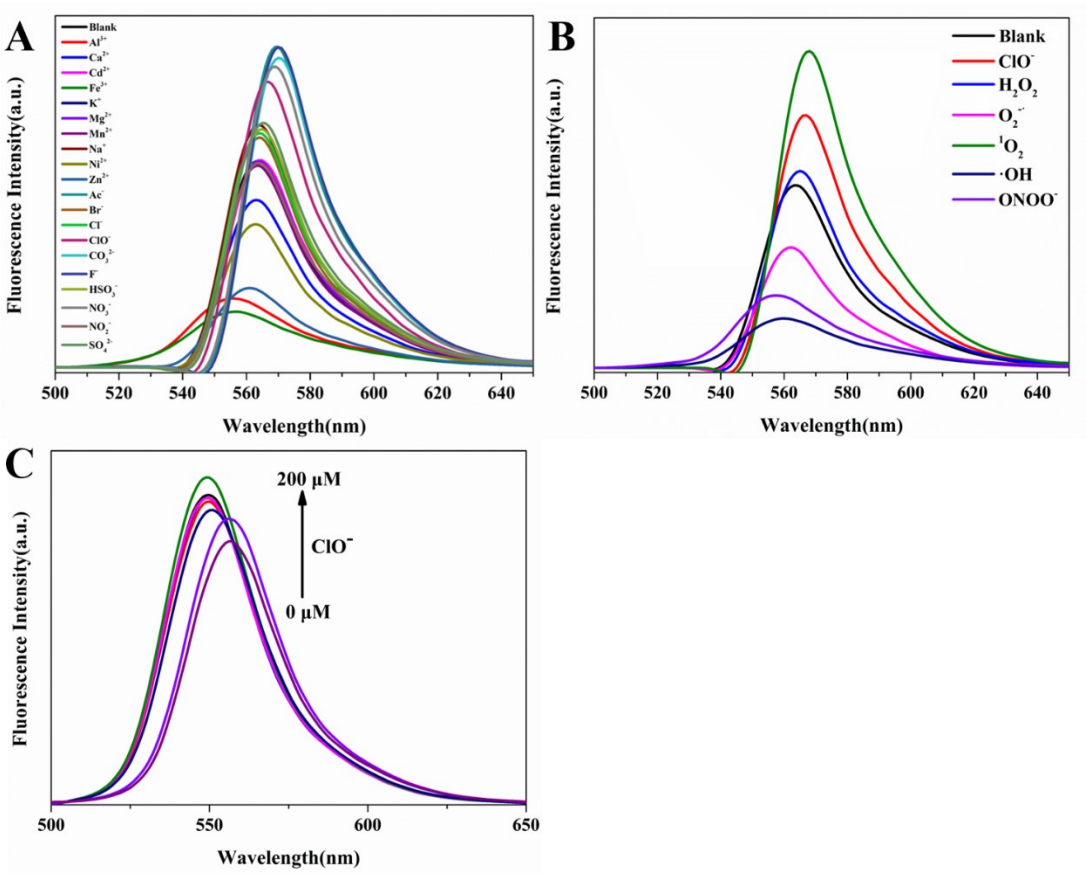

Figure S7. (A) Fluorescence response of EY (50μg/mL) toward various ions (10 mM) and (B) toward various ROS species (50 μM (ClO-, O_2, OH·, $ONOO^-$), 50 mM H_2O_2, 5 mM $O_2^{-\cdot}$). (C) Fluorescence response of EY toward various amount of ClO^-. λ_{ex} =467 nm, slid width, 1.5nm/3nm.

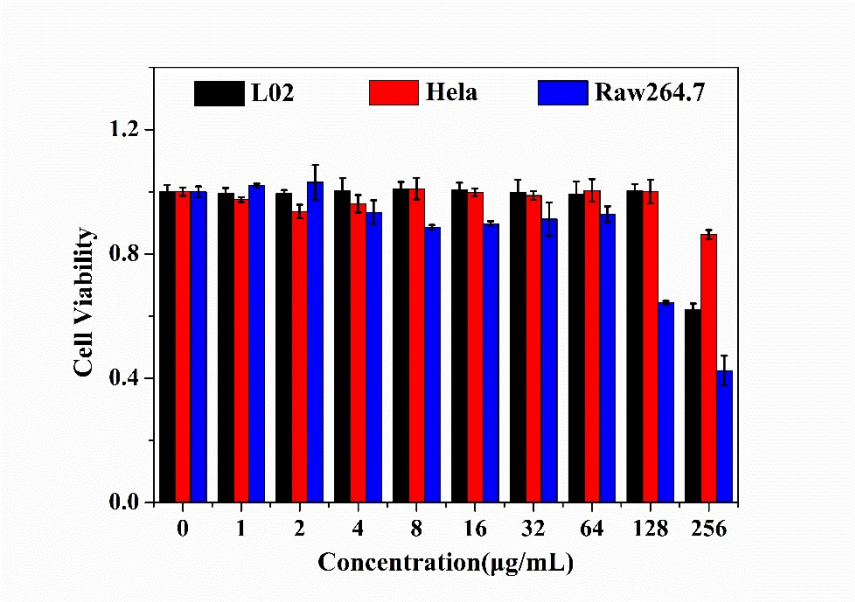

Figure S8. Viability of L02, Hela and Raw264.7 cells after incubated with various concentrations of EY/UiO-66-NH_2 after 24 h.

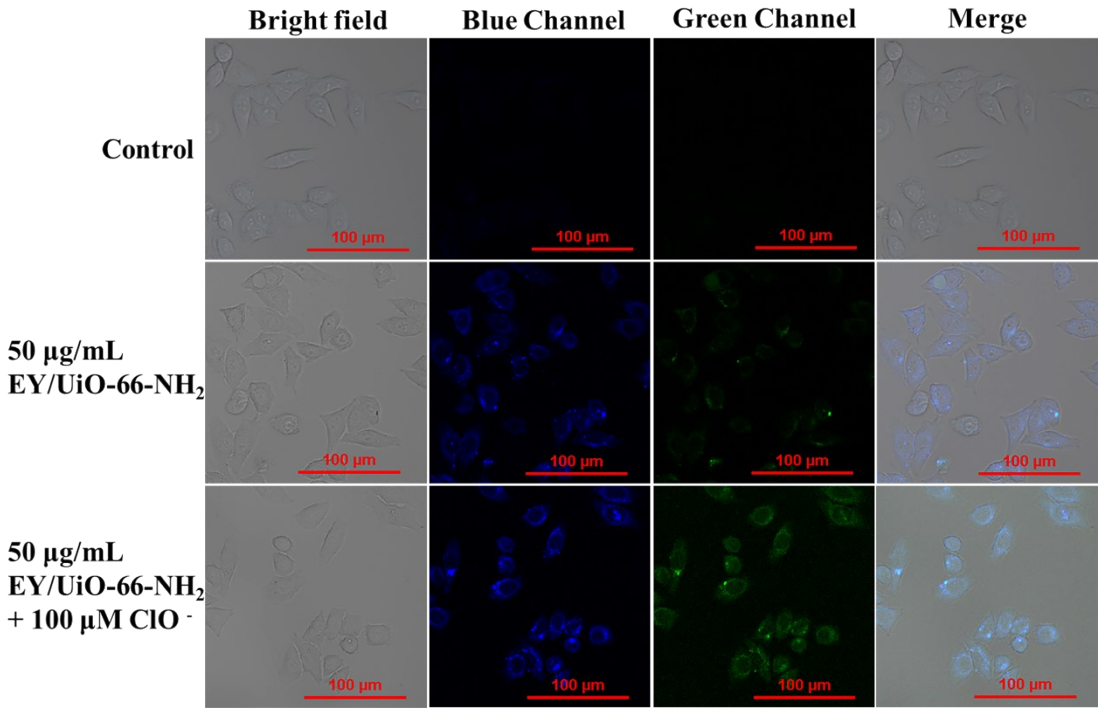

Figure S9. Confocal fluorescence imaging of exogenous ClO^- in L02 cells. (A) Bioimaging of L02 cells without any treatment; (B) Bioimaging of L02 cells incubated with EY/UiO-66-NH_2 (50 μg/mL) for 5 hours at 37°C and (C) further incubated with 100 μM NaClO for 2h.

Table S2. Comparison of different sensors for hypochlorite sensing

Probe	Output signal	Detection limit (nM)	Linear range (μM)	Ref
UiO-68-ol	OFF	100	0.1-100	3
{[Eu_2Cu (IN)$_5$(CO_3) (H_2O)]}	OFF	10000	10-400	4
AF@MOF801	OFF	52	0-7	5
UiO-68-PT	ON	280	0-80	6
AuNCs@NMOF	ON	30	0.08-1000	7
CD/CCM@ZIF-8	Ratiometric, FRET	67	0.1-50	8
PDA/Eu/PDA-UiO-66-NH_2 (x)	Ratiometric, ON	100	0.1-60	9
NH_2-MIL-53(Al)	OFF	40	0.05-15	10
PDA-EuBBA-PEG-DBA-Fe_3O_4@ZIF-8	OFF	0.133	0-100	11
Hf-UiO-66-(NH_2)$_2$ MOF	OFF	9	100-1000	12
NH_2-Cu-MOF	OFF	360	0-12.5	13
UiO-66-NH_2	Ratiometric, ON	63.8	0.1-150	14
EY/UiO-66-NH_2	Ratiometric, ON	46.4	0.1-200	This work

References

1 Y. J. Ma, G. H. Xu, F. D. Wei, Y. Cen, X. M. Xu, M. L. Shi, X. Cheng, Y. Y. Chai, M. Sohail, and Q. Hu, ACS Appl. Mater. Interfaces. 2018, **10**, 20801-20805.

2 P. F. Xing, K. Gao, B. Wang, J. Gao, H. Yan, J. Wen, W. S. Li, Y. Q. Xu, H. J. Li, J. X. Chen, W. Wang and S. G. Sun, 2016, **52**, 5064-5066.

3 Y. A. Li, S. Yang, Q. Y. Li, J. P. Ma, S. Zhang, Y. B. Dong, Inorg. Chem. 2017, **56**, 13241-13248.

4 H. Xu, C. S. Cao, J. Z. Xue, Y. Xu, B. Zhai, B. Zhao, Chem.-Eur. J. 2018, **24**, 10296.

5 Y. Ye, L. Zhao, S. Hu, A. Liang, Y. Li, Q. Zhuang, G. Tao, J. Gu, Dalton Trans. 2019, **48**, 2617- 2625.

6 Q. Y. Li, Y. A. Li, Q. Guan, W. Y. Li, X. J. Dong, Y. B. Dong, Inorg. Chem. 2019, **58**, 9890-9896.

7 X. Cao, S. Cheng, Y. You, S. Zhang, Y. Xian, Anal. Chim. Acta. 2019, **1092**, 108-116.

8 H. Tan, X. Wu, Y. Weng, Y. Lu, Z. Z. Huang, Anal. Chem. 2020, **92**, 3447-3454.

9 Y. N. Zeng, H. Q. Zheng, X. H. He, G. J. Cao, B. Wang, K. J. Wu, Z. J. Lin, Dalton Trans., 2020, **49**, 9680-9688.

10 C. R. Li, J. Hai, S. L. Li, B. D. Wang, Z. Y. Yang, Nanoscale, 2018, **10**, 8667-8676.

11 T. Lu, L. Zhang, M. Sun, D. Deng, Y. Su and Y. Lv, Anal. Chem. 2016, **88**, 3413–3420.

12 S. Nandi, S. Biswas, Microporous and Mesoporous Materials. 2020, **299**, 110116.

13 P. P. Huo, Z. J. Li, C. B. Fan, S. Z. Pu, New J. Chem., 2020, **44**, 19753.

14 F. F. Yu, T. Y. Du, Y. H. Wang, C. M. Li, Z. J. Qin, H. J. Jiang, X. M. Wang, Sensors & Actuators: B. Chemical. 2022, **353**, 131032.